Pamukkale Univ Muh Bilim Derg, 31(8), 1391-1398, 2025
(Special Issue of the 10th Geochemistry Symposium)

Pamukkale Üniversitesi Mühendislik Bilimleri Dergisi

Pamukkale University Journal of Engineering Sciences

Spatial distribution and risk assessment of potential environmentally hazardous elements in coal: a case study of the Central Anatolia coalfields

Kömürdeki çevreye zararlı olabilecek elementlerin mekânsal dağılımı ve risk değerlendirmesi: Orta Anadolu kömür sahaları için örnek bir çalışma

Neslihan Ünal Kartal[1*], *Cevdet Bertan Güllüdağ*[2]

[1]Gölhisar School of Applied Sciences, Burdur Mehmet Akif Ersoy University, Burdur, Türkiye.
nunal@mehmetakif.edu.tr
[2]Vocational School of Technical Science, Akdeniz University, Antalya, Türkiye.
bgulludag@akdeniz.edu.tr

Received/Geliş Tarihi: 20.09.2025 Revision/Düzeltme Tarihi: 24.10.2025 doi: 10.65206/pajes.30388
Accepted/Kabul Tarihi: 04.11.2025 Special Issue Article/Özel Sayı Makalesi

Abstract

A wide range of environmental risks may arise during coal mining. At the same time, it is possible that during the transportation and extraction of coal, locals and especially the workers working in the mining area may be harmed, depending on their proximity to agricultural lands and settlement centers. Revealing the spatial distribution of potentially hazardous elements in coal (Ag, As, B, Ba, Be, Cd, Cl, Co, Cr, Cu, F, Hg, Mn, Mo, Ni, P, Pb, Sb, Se, Sn, Th, Tl, U, V, Zn) is an important step for identifying potential environmental health risks. Using Geographic Information System (GIS) tools and Remote Sensing techniques, the objective of this study is to identify and compare the spatial risk assessment of the elements in the Ilgın (Konya) and Karapınar (Konya) lignite areas. The surroundings of the mining sites were classified into 7 classes (crops, rangeland, bare ground, water, built area, flooded vegetation, trees) using SENTINEL-2 satellite data with a 10 m spatial resolution and CORINE LULC data. Subsequently, mapping and buffer zone analyses were conducted using the GIS. The land use land cover classification revealed that both mining sites were highly distributed in agricultural lands (Karapınar: 155.32 km², Ilgın: 178.45 km²) and rangeland (Karapınar: 140.4 km², Ilgın: 40.72 km²). Geochemical results showed that Ni concentrations exceeded the limit values in the Karapınar lignites, while As concentrations exceeded the limit values in the Ilgın lignites. Based on these results, it was concluded that the Ni concentration in agricultural lands and rangelands around the Karapınar site, and the As concentration in agricultural lands and rangelands around the Ilgın site, should be monitored periodically.

Keywords: LULC, Sentinel-2, CORINE, Lignite.

Öz

Kömür madenciliği faaliyetleri sırasında çok çeşitli çevresel risk unsurları ortaya çıkabilmektedir. Aynı zamanda kömürün çıkarılması ve taşınması sırasında maden sahasında çalışan işçiler başta olmak üzere tarım arazileri ve yerleşim merkezlerine yakınlık düzeyine göre bölge halkı olumsuz etkilenebilmektedir. Kömürdeki çevreye zararlı olabilecek elementlerin (Ag, As, B, Ba, Be, Cd, Cl, Co, Cr, Cu, F, Hg, Mn, Mo, Ni, P, Pb, Sb, Se, Sn, Th, Tl, U, V, Zn) mekansal dağılımlarını ortaya koymak, çevre sağlığı açısından potansiyel risklerin belirlenmesi için önemli bir adımdır. Bu çalışmada Uzaktan Algılama yöntemleri ve Coğrafi Bilgi Sistemleri (CBS) araçları ile Ilgın (Konya) ve Karapınar (Konya) linyit sahalarındaki elementlerin mekansal risk değerlendirilmesinin tespit edilmesi ve karşılaştırılması amaçlanmıştır. Maden sahalarının çevresi 10 m mekansal çözünürlüğe sahip SENTINEL-2 uydusu ile CORINE LULC verileri kullanılarak 7 sınıfa (tarım arazileri, mera, çıplak arazi, su, yapılaşmış alanlar, sulu bitki örtüsü, ağaçlık alanlar) ayrılmıştır. Ardından CBS ile haritalama ve tampon bölge analizleri yapılmıştır. Arazi Kullanımı/Arazi Örtüsü ile tespit edilen sınıflamada her iki maden sahasının da tarım arazilerinde (Karapınar: 155.32 km²; Ilgın: 178.45 km²) ve mera alanlarında (Karapınar: 140.4 km²; Ilgın: 40.72 km²) yüksek dağılım gösterdiği tespit edilmiştir. Jeokimyasal bulgular ile Karapınar linyitlerinde Ni, Ilgın linyitlerinde ise As konsantrasyonları sınır değerlerin oldukça üzerinde sonuçlar vermiştir. Elde edilen bu bulgular ile tarım arazileri ve mera alanlarında, Karapınar sahasında Ni, Ilgın sahasında As konsantrasyonlarının belirli aralıklarla kontrol edilmesi gerekebileceği sonucuna varılmıştır.

Anahtar kelimeler: LULC, Sentinel-2, CORINE, Linyit.

1 Introduction

Despite increasing investments in renewable energy, coal remains a significant energy source both in Türkiye and globally. It is particularly prominent in developing countries as a cheap and reliable source of electricity generation. Although the share of renewable energy in Türkiye has increased in recent years, coal still accounts for a significant portion of energy production due to the country's rich lignite reserves. According to the 2024 Coal Sector Report [1], coal accounted for 40.12 Mtoe of Türkiye's total primary energy supply, ranking third after oil and natural gas. Nevertheless, the extensive use of coal has important environmental consequences, as toxic elements such as As, Hg, Pb, Cd, and Ni may be released during its extraction, storage, and combustion, contaminating soil and water resources and posing risks to ecosystems and human health.

Various studies have been conducted on the geochemical properties of coal in the Ilgın (Konya) and Karapınar (Konya) coalfields, two important coal basins in Central Anatolia (Figure 1). Altunsoy et al. [2],[3] and Karadirek et al. [4] determined the concentrations of potentially harmful elements in coal and discussed their environmental impacts. However, in these studies, the environmental risks in mining areas were not spatially associated with land-use classifications.

*Corresponding author/Yazışılan Yazar

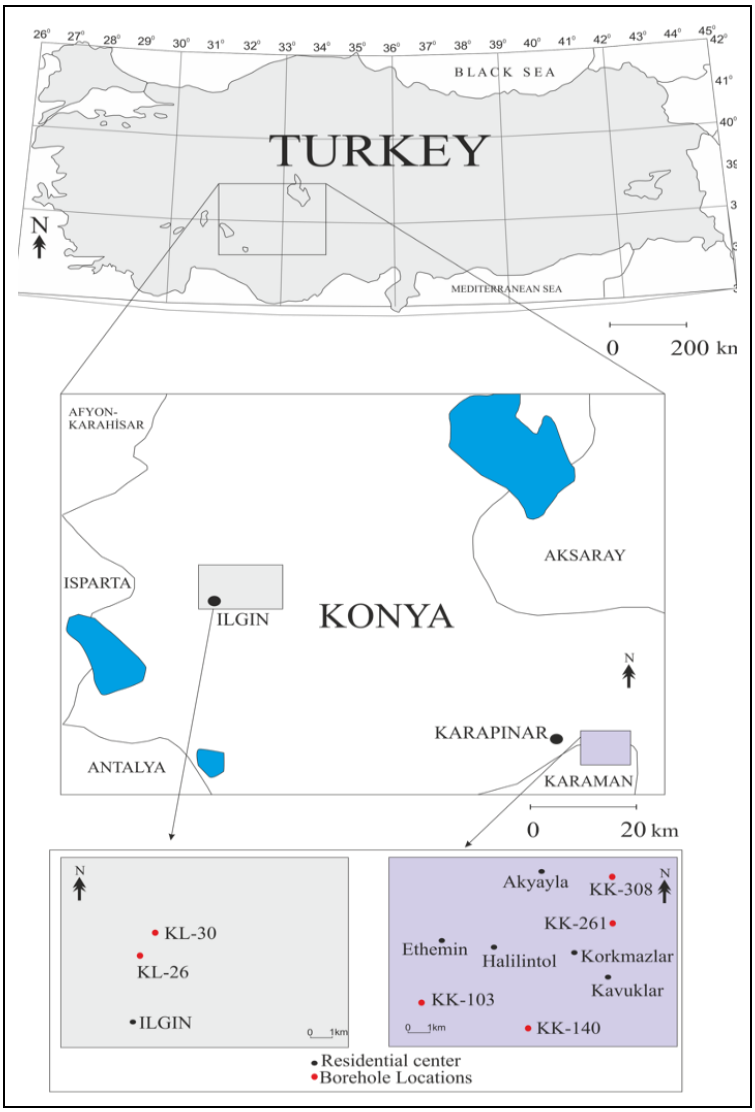

Figure 1. Location map of study areas.

This study aims to reveal the distribution of the effects of coal mining on residential areas, agricultural lands, and natural ecosystems. In this context, existing geochemical data and satellite-based land classifications were evaluated together.

Advancements in satellite remote sensing technology have revolutionized the way Earth's surface is monitored. The Copernicus Program, developed by the European Space Agency (ESA) and the European Union (EU), has significantly enhanced Earth observation by providing Sentinel-2 multispectral products [5].

Accurate, real-time land use/land cover (LULC) maps are essential for delivering the precise information needed to monitor, plan, and manage the dynamic Earth system [6]. Information on LULC, including forest cover, plays a crucial role in the development of land planning and management strategies. Satellite remote sensing (RS) data with varying resolutions have become a valuable source of information, enabling more reliable predictions than traditional inventory methods [7].

The fundamental strength of Geographic Information Systems (GIS) lies in the integrated analysis of spatial and attribute data. Attribute data are typically collected through sampling. The values of these data can then be extended to unsampled areas using interpolation methods [8]. In spatial interpolation, weighted-average techniques are often used, and the proper selection of neighbors is significant for accuracy [9]. Buffer analysis is also regarded as one of the key functions of spatial analysis in GIS [10].

2 Geological setting

Neogene basins in Central Anatolia were formed as a result of tectonic regimes triggered by plate collisions during the Cenozoic [11],[12]. Lacustrine and telmatic depositional environments that developed during the Late Miocene–Pliocene created favorable conditions for lignite formation, leading to the development of significant lignite accumulation areas in the region [13-15]. Among these basins are the Ilgın and Karapınar coalfields.

The Karapınar coalfield and its surroundings are formed by the Berendi Formation, which consists of Jurassic-Cretaceous crystalline limestone and dolomitic limestone [16]. Overlying this basement, the Insuyu Formation consists of Upper Miocene-Pliocene sandstone, siltstone, mudstone, claystone, and clayey limestone. The Insuyu Formation conformably transitions into the Pliocene Hotamış Formation, which contains sandstone, siltstone, mudstone, claystone, and coal levels. The youngest unit in the area is Quaternary alluvium, consisting of clays containing silt and tuff in places (Figure 2).

The bedrock in the Ilgın coal basin consists of Palaeozoic–Mesozoic crystalline limestone, quartzite, and metamorphic rocks (Figure 3). The Miocene Çiğil Formation unconformably overlies this bedrock. The Çiğil Formation consists of conglomerate, sandstone, siltstone, claystone, mudstone, marl, limestone, and coal levels. The Pliocene Dursunlu Formation conformably overlies the Çiğil Formation. The Dursunlu Formation, which also contains the lignite deposits covered by this study, consists of sandstone, siltstone, claystone, marl, and coal. All these units are unconformably covered by Quaternary slope debris, fan deposits, and alluvium [2].

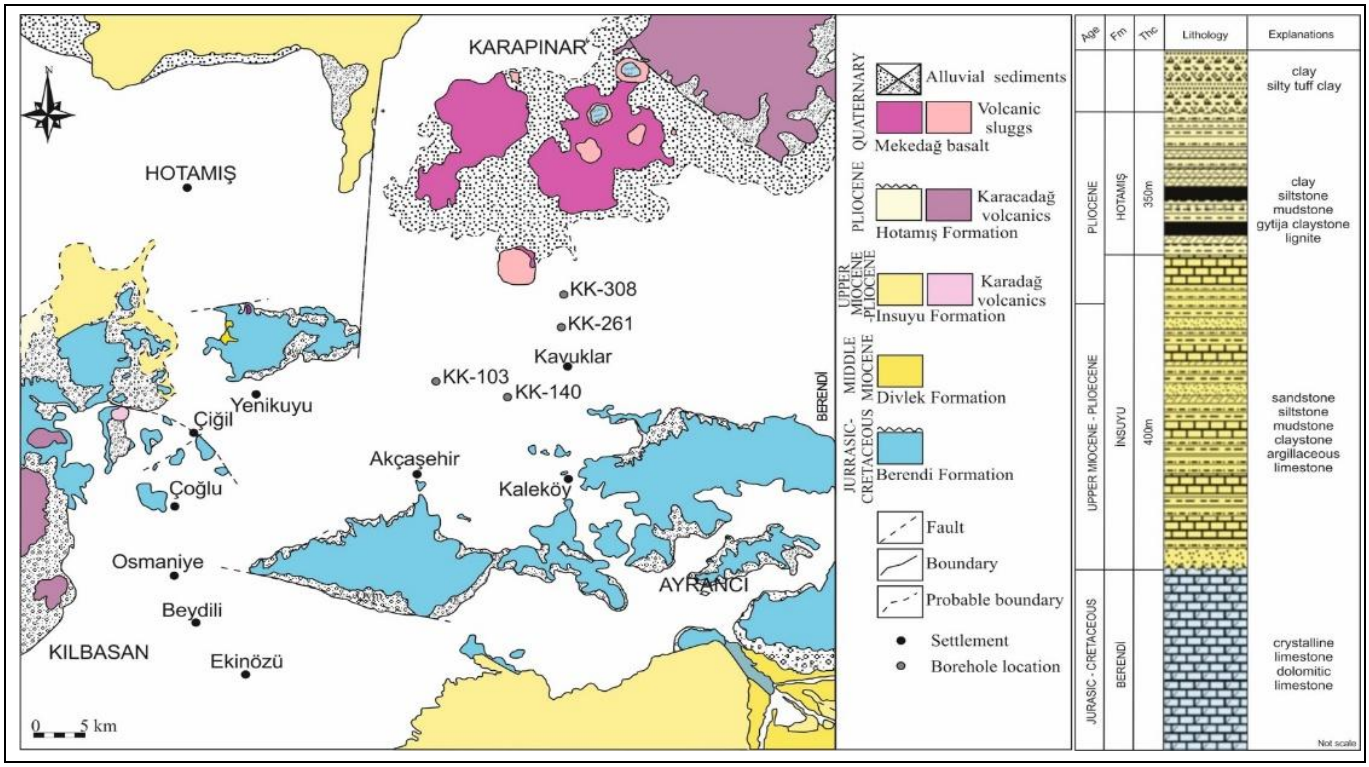

Figure 2. Geological map (modified from [19]) and generalized stratigraphic section of the Karapınar area [20].

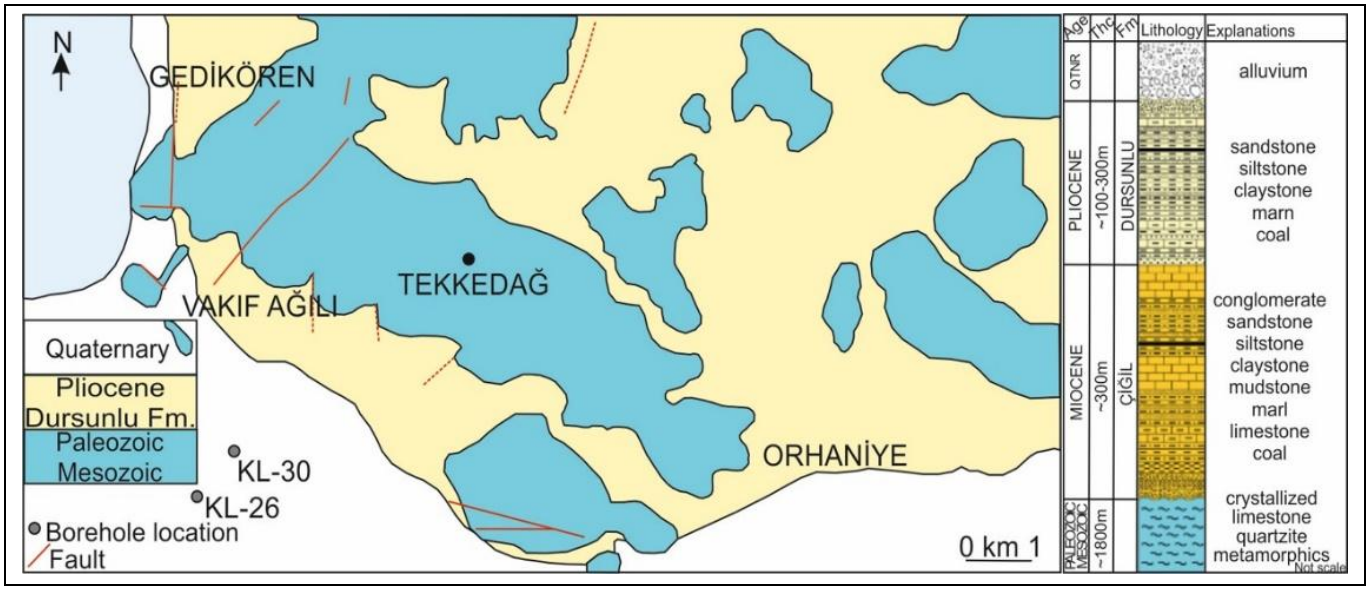

Figure 3. Geological map and generalized stratigraphic section (modified from [21]) of the Ilgın area [3].

3 Materials and methods

In this study, a total of 47 lignite samples were considered, including 21 samples from four boreholes in the Karapınar coalfield and 26 samples from two boreholes in the Ilgın coalfield. Elemental concentrations in these samples had been previously determined in the same laboratory using identical protocols based on ICP-MS and ICP-AES techniques.

Spatial analyses were carried out in two stages using RS methods and GIS tools. In the RS stage, Sentinel-2 satellite images obtained from the ArcGIS Living Atlas of the World, an open-access source provided by ESRI, were utilized (Figure 4). The ArcGIS Living Atlas of the World platform, offered free by ESRI, provides LULC maps at 10 m resolution using Sentinel-2 satellite imagery.

In this study, the Sentinel-2 Level-2A surface reflectance data were selected from cloud-free images acquired during the summer season of 2023 (June–August). This period was preferred because it corresponds to the time when agricultural activities are at their peak and vegetation classes (crops, rangeland, flooded vegetation) are most clearly distinguishable. The images were obtained from the ArcGIS Living Atlas of the World platform, which automatically provides the most up-to-date cloud-masked mosaics through the ESA Sentinel Hub infrastructure. The CORINE LULC data were derived from the 2018 dataset published by the Copernicus Land Monitoring Service. This dataset is standardized across Europe, has a spatial resolution of 100 m, and demonstrates a high overall accuracy exceeding 85%. Both datasets were spatially aligned (resampled), and all spatial analyses were performed within the same coordinate reference system (WGS 84/UTM Zone 36N) to ensure geospatial consistency [17]. The purpose of this analysis was to classify land into LULC categories. LULC includes datasets at both global and regional scales that describe the physical forms of land observed on Earth's surface and their use under natural or human influence. These maps are generated by a deep learning model trained with over 20,000 sample sites and more than five billion manually labeled Sentinel-2 pixels, using visible blue, green, red, near-infrared, and two shortwave infrared bands from Sentinel-2 L2A surface reflectance data [17],[18]. The use of these data enables the production of a detailed thematic land-use map comprising nine classes. The platform's classes, along with their descriptions, are presented in Table 1. In this study, land classification was performed using the methods described above.

Figure 4. Esri–Sentinel-2 LULC ArcGIS Living Atlas of the World platform [18]

Table 1. Land Use/Land Cover class definitions [17].

Class	Description
Water	Areas that contain water throughout the year may not include regions with irregular or temporary water presence: rivers, ponds, lakes, oceans, or salt flats.
Trees	Areas with tall and dense vegetation. Forests, plantations, wetlands.
Flooded Vegetation	Seasonally inundated areas consisting primarily of grasses, shrubs, trees, and bare soil mixtures; floating vegetation, rice paddies, and other intensively irrigated and flooded agricultural lands.
Crops	Cultivated areas planted by humans with cereals, grasses, and non-tree crops; maize, wheat, soybeans, and fallow agricultural fields within structured land.
Built area	Man-made structures: major road and railway networks, houses, densely populated villages/towns/cities, paved roads.
Bare Ground	Rock or soil surfaces with little or no vegetation cover throughout the year; exposed rock or soil, deserts, and dunes, dry salt flats, dried lakebeds, and mining areas.
Snow/Ice	Large areas of permanent glaciers, snow cover, and snowfields.
Clouds	Land cover information unavailable due to persistent cloud cover.
Rangeland	Open areas covered with uniform low vegetation. Natural grasslands and fields, parks, golf courses, lawns, pastures, and moderately sparse shrubs.

In the second stage of spatial analysis, buffer and interpolation analyses were conducted using GIS tools. The open-source software QGIS was employed for this purpose. QGIS is used for the collection, storage, editing, analysis, and mapping of geographic information. It offers users a wide range of tools for processing, visualizing, and analyzing data. Through the capabilities it provides, complex geographic data can be effectively managed and analyzed. Particularly in GIS-based analyses, QGIS's robust, flexible tools enable users to examine data in detail and present results visually.

Since the datasets were obtained from different sources (geological maps, CORINE LULC data, Sentinel-2 satellite imagery, and sampling coordinates), a geographic reprojection process was first performed, followed by georeferencing using QGIS software. Through this procedure, all raster and vector datasets were analyzed within the same spatial reference framework, ensuring geospatial consistency. As a result, no positional displacement or scale discrepancies occurred during buffer, interpolation, and thematic overlay analyses.

4 Results and discussion

The average concentrations of potentially harmful elements in coal samples from the Karapınar and Ilgın fields are presented in Table 2.

Table 2. Element concentrations of Karapınar and Ilgın coals.

Elements	Karapınar[a]	Ilgın[b]	World[c]	UCC[d]
P*	0.034	0.017	0.02	0.07
Mn*	0.036	0.025	0.01	0.08
Cr	180	80	15	92
Ba	172.58	397.70	150	624
Be	0.59	2.43	1.20	2.10
Co	13.45	7.82	4.20	17.30
Sn	0.80	2.74	0.79	2.10
Th	4.53	11.19	3.30	10.50
U	4.55	4.97	2.90	2.70
V	59.55	69.71	22	97
Mo	2.90	1.40	2.20	1.10
Cu	13.99	13.01	15	28
Pb	12.17	16.27	6.6	17
Zn	25.58	44.86	18	67
Ni	112.02	13.60	9	47
As	16.05	74.98	7.6	4.80
Cd	0.24	0.18	0.24	0.09
Sb	0.25	0.18	0.84	0.40
Hg	0.02	0.06	0.10	0.05
Tl	0.10	0.10	0.68	0.90
Se	1.00	0.90	1.00	0.09

[a][2],[3], [b][4], [c]World brown coal [25], [d][26]. * Elements are in %, others in ppm.

The Ag was not included in the assessment as it remained below the detection limit (0.1 ppm) in most samples. The concentrations of Cd, Sb, and Tl are lower in both fields compared to the upper continental crust (UCC) and world low-rank coal averages. The concentrations of Ba, Co, Sn, Th, U, V, Pb, Zn, Ni, and As are higher in both fields compared to the world low-rank coal averages. Of these elements, U and Mo at the Karapınar site, and Sn, Th, U, and Mo at the Ilgın site, have concentrations higher than the UCC but are close to average values. However, Ni concentrations in the Karapınar area and As concentrations in the Ilgın area are significantly above both global and UCC values. In the EU [22], the upper threshold values for these elements in agricultural soils are 75 mg/kg (Ni) and 25.5 mg/kg (As), and the measured concentrations exceed these limits. Previous studies have demonstrated the presence of pyrite in both the Karapınar [23] and Ilgın [13] coalfields. According to the literature [24], Ni in coal is generally associated with clay minerals, organic matter, and sulfides, whereas As is typically related to pyrite and organic matter under reducing conditions. These factors may help explain the elevated Ni and As concentrations observed in the study area.

Using Sentinel-2 satellite images and CORINE data, the study areas were classified into seven categories: crops, rangeland, bare ground, water, built area, flooded vegetation, and trees. In the Karapınar area, 155.32 km^2 of crops and 140.40 km^2 of rangeland constitute the two largest land classes (Table 3 and Figure 5). In the Ilgın area, 178.45 km^2 of crops and 40.72 km^2 of rangeland also stand out among the land classes (Table 3 and Figure 6).

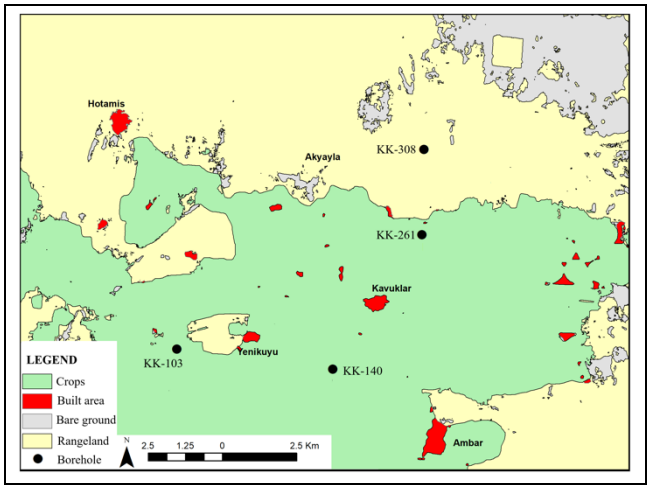

Figure 5. LULC classes and borehole locations in the Karapınar coalfield.

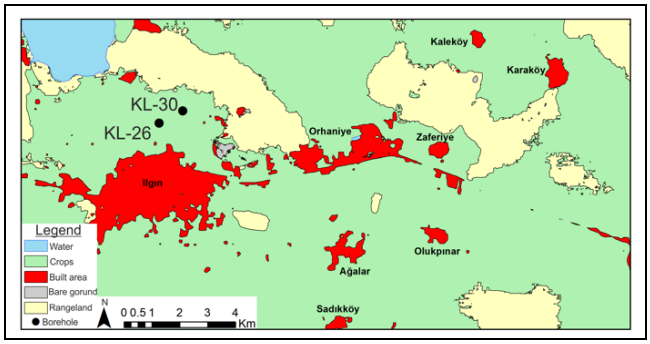

Figure 6. LULC classes and borehole locations in the Ilgın coalfield.

Table 3. LULC attributes and fields.

Classes	Karapınar (km^2)	Ilgın (km^2)
Water	-	5.76
Crops	155.32	178.45
Built area	2.50	18.16
Bare ground	20.91	0.30
Rangeland	140.4	40.72

Since flooded vegetation and tree areas are absent at both sites, these classes were not included in the table.

GIS-based buffer zone analyses have numerically determined the environmental impact area of mining activities, as shown in Table 4.

Table 4. Buffer zones and land use attributes.

Study area	Buffer zones(m)	Crops	Range land	Bare ground	Built area
Ilgın	250	0.38	-	-	-
	500	1.56	-	-	-
	1000	6.03	0.19	-	0.048
Karapınar	250	1.52	0.57	-	-
	500	6.30	2.26	0.20	-
	1000	25.42	8.91	0.02	0.08

In the Ilgın field, there is 0.38 km^2 of crops within the 250 m buffer zone, increasing to 1.56 km^2 at 500 m and 6.03 km^2 at 1000 m. In addition to crops, 0.19 km^2 of rangeland and 0.048 km^2 of built area are affected in the 1000 m buffer zone of this field. These values show that agricultural activities in the Ilgın field are particularly sensitive to pollutants from coal mining.

This effect was found to be more pronounced in the Karapınar area. Within the 250 m buffer zone, there are 1.52 km^2 of crops and 0.57 km^2 of rangeland, while at 500 m, there are 6.30 km^2 of crops and 2.26 km^2 of rangeland. Within the 1000 m buffer zone, there are 25.42 km^2 of crops and 8.91 km^2 of rangeland. In addition, 0.08 km^2 of built area is also affected. These findings, together with the high coal reserves in the Karapınar field, indicate that the potential risk in the Karapınar field is much higher than in the Ilgın field. Furthermore, the fact that residential areas are located within the impact zone of mining activities in both fields indicates that these activities may pose a direct risk to the health of the local population.

Interpolation maps have been created for the Ni (Karapınar) and As (Ilgın), which carry a high-risk potential (Figures 7 and 8). It has been determined that the areas with the highest concentrations of these elements coincide exactly with those where agriculture and livestock farming are carried out. The literature [27]-[31] indicates that elements such as As and Ni in coal cause various diseases and have the potential to accumulate in the ecosystem. Even though the number of people exposed to As released from coal combustion or coal and its by-products is relatively small, As is considered the coal-derived element that causes the most health problems and deaths [24]. Similarly, Ni, detected at high concentrations in Karapınar coal, is known to pose a high environmental risk for respiratory disorders and carcinogenic effects [32],[33]. This indicates that soil and water quality must be monitored regularly in both areas.

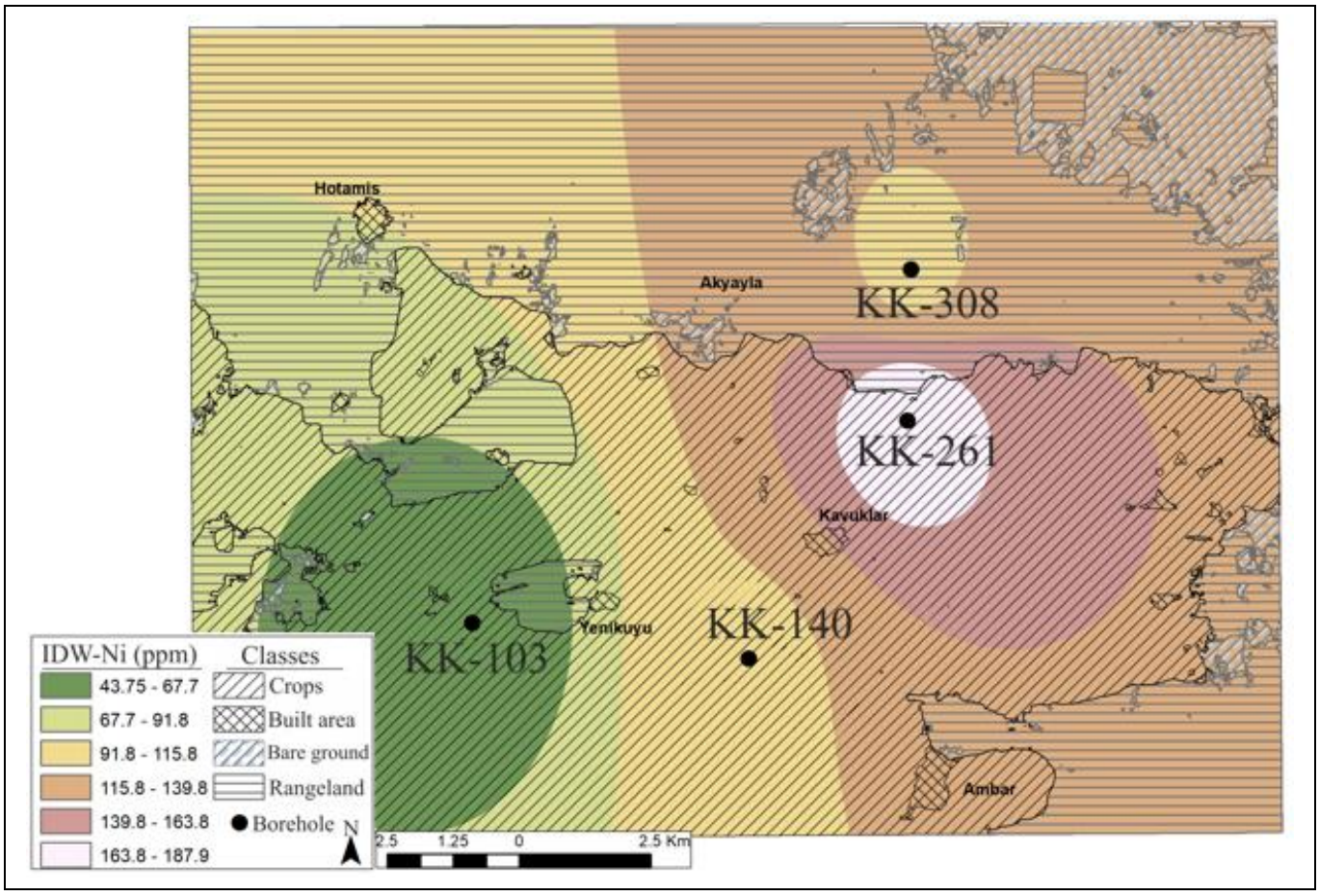

Figure 7. Interpolation map of Ni distribution in the Karapınar coalfield, overlaid with LULC classes.

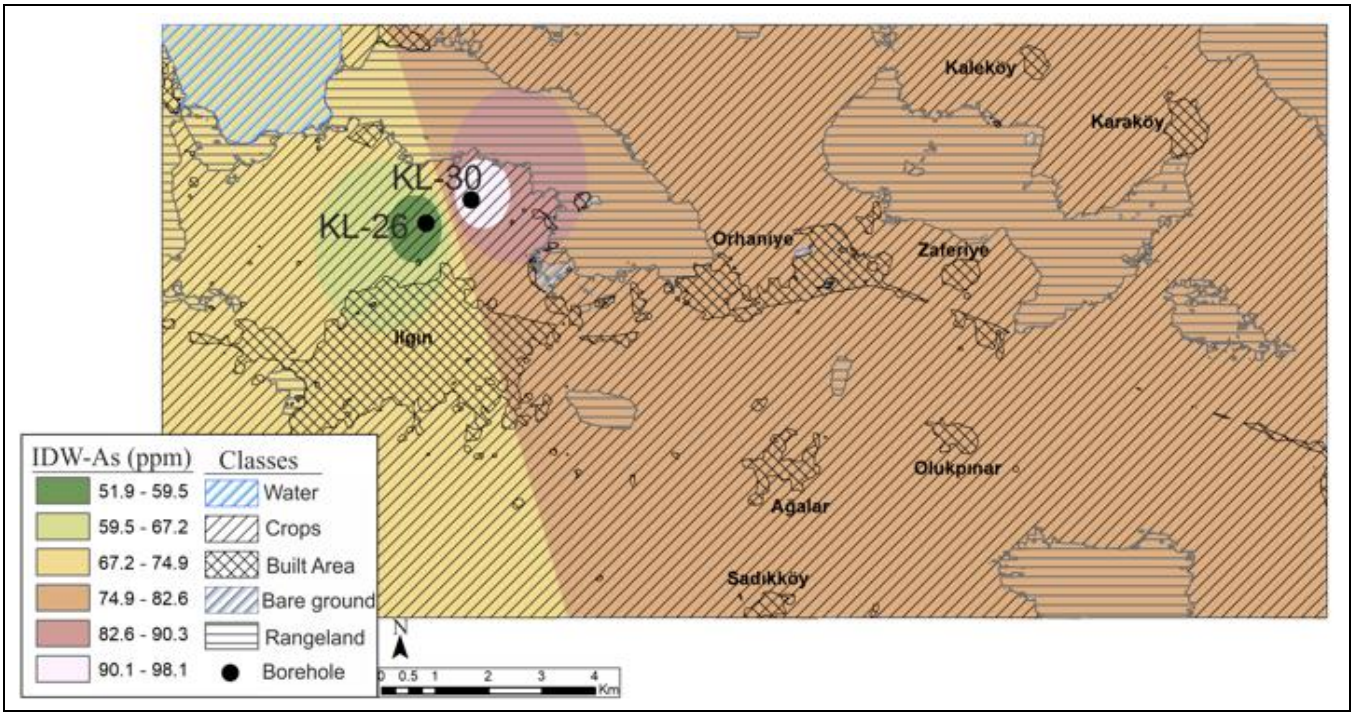

Figure 8. Interpolation map of As distribution in the Ilgın coalfield, overlaid with LULC classes.

5 Conclusions

The concentrations of Ni and As in the Karapınar coalfield and the Ilgın coalfield significantly exceed both the global average for low-rank coal and the UCC average. In Karapınar, the average Ni concentration (112 ppm) is approximately 2.4 times higher than the UCC value (47 ppm), while in Ilgın, the average As concentration (75 ppm) is more than 15 times higher than the UCC value (4.8 ppm). By combining geochemical data with RS and GIS analyses, the spatial extent of Ni and as contamination was determined, allowing the risk to be evaluated in relation to land use. GIS-based spatial analyses have shown that the areas most affected by mining activities in both fields are agricultural land and rangeland. In Karapınar, 25.42 km^2 of crops and 8.91 km^2 of rangeland within a 1000 m buffer zone, and in Ilgın, 6.03 km^2 of crops and 0.19 km^2 of rangeland are at risk. This situation reveals that mining activities may have adverse health effects on food production. If the current mining activities and planned thermal power plant projects in the region are implemented, there is a risk of high concentrations of potentially polluting elements being released into the environment. Therefore, soil, water, and air quality in the affected areas should be monitored seasonally using standard environmental sampling methods, particularly for Ni and As, as well as other potentially hazardous elements. In addition, strict measures should be taken to control dust during mining activities.

6 Author contribution statements

In the present study, Neslihan Ünal Kartal contributed to the study design, literature review, and manuscript writing; Cevdet Bertan Güllüdağ contributed to the conceptualization of the idea, the implementation of the analyses, writing, and the critical review of the manuscript.

7 Statement of ethical committee approval and conflict of interest

"Ethics committee approval was not required for the preparation of this article".

"The authors declare no conflict of interest with any individual or institution in relation to the preparation of this article."

8 References

[1] Turkish Coal Enterprises (TKİ). "Coal (Lignite) Sector Report 2024". Ankara, Türkiye, 2025.

[2] Altunsoy M, Ozcelik O, Ozdogan M, Güllüdağ CB. "Major and trace element contents in coaly units of the Pliocene Dursunlu Formation". *Procedia Earth and Planetary Science*, 15, 774-780, 2015.

[3] Altunsoy M, Özçelik O, Güllüdağ CB. "Comparision of major and trace element enrichments of Pliocene coal fields from Karapınar and Ilgın (Konya) Basins (Turkey). *Journal of Scientific and Engineering Research*, 4(10), 269-275, 2017.

[4] Karadirek S, Ünal N, Özçelik O, Altunsoy M. "Potential health and environmental effects of trace elements in Karapınar (Turkey) coals". *1th International Conference on advances in Engineering Sciences*, Phuket, Thailand, 15-19 May 2017.

[5] Phiri D, Simwanda M, Salekin S, Nyirenda VR, Murayama Y, Ranagalage M. "Sentinel-2 data for land cover/use mapping: a review". *Remote Sensing*, 12(14), 2291, 2020.

[6] Nasiri V, Deljouei A, Moradi F, Sadeghi SMM, Borz SA. "Land use and land cover mapping using Sentinel-2, Landsat-8 satellite images, and google earth engine: a comparison of two composition methods". *Remote Sensing*, 14(9), 1977, 2022.

[7] Nguyen HTT, Doan TM, Tomppo E, McRoberts RE. "Land use/land cover mapping using multitemporal sentinel-2 ımagery and four classification methods-a case study from Dak Nong, Vietnam". *Remote Sensing*, 12(9), 1367, 2020.
[8] Sárközy F. "GIS functions-interpolation". *Periodica Polytechnica Civil Engineering*, 43(1), 63-87, 1999.
[9] Gold CM. *Surface Interpolation, Spatial Adjacency and GIS*. Editor: Raper J. Three Dimensional Applications in GIS, 21-25, London, England, CRC Press, 2020.
[10] Dong P, Yang C, Rui X, Zhang L, Cheng Q. "An effective buffer generation method in GIS". *IEEE International Geoscience and Remote Sensing Symposium*, Toulouse, France, 21-25 July 2003.
[11] Görür N, Tüysüz O, Şengör, AMC. "Tectonic evolution of the central Anatolian basins". *International Geology Review*, 40(9), 831-850, 1998.
[12] Schildgen TF, Yıldırım C, Cosentino D, Strecker MR. "Linking slab break-off, Hellenic trench retreat, and uplift of the Central and Eastern Anatolian plateaus". *Earth-Science Reviews*, 128, 147-168, 2014.
[13] Karayigit AI, Akgun F, Gayer RA, Temel A. "Quality, palynology, and palaeoenvironmental interpretation of the Ilgin lignite, Turkey". *International Journal of Coal Geology*, 38(3-4), 219-236, 1999.
[14] Akgün F, Olgun E, Kuşçu İ, Toprak V, Göncüoğlu MC. "New data on the stratigraphy, depositional environment, and real age of the Oligo-Miocene cover of the central Anatolian crystalline complex". *Bulletin of Turkish Association of Petroleum Geology*, 6, 51-68, 1995.
[15] Toprak S. "Petrographic properties of major coal seams in Turkey and their formation". *International Journal of coal geology*, 78(4), 263-275, 2009.
[16] Karadirek S, Altunsoy M. "Geochemical characteristics and paleodepositional setting of coal-bearing strata in Konya-Karapınar Basin, Central Anatolia, Turkey". *Journal of African Earth Sciences*, 186, 104443, 2022.
[17] Karra K, Kontgis C, Statman-Weil Z, Mazzariello JC, Mathis M, Brumby SP. "Global land use/land cover with Sentinel-2 and deep learning". In Proceedings of the IGARSS 2021-*2021 IEEE International Geoscience and Remote Sensing Symposium*, Brussels, Belgium, 11–16 July 2021.
[18] Özgürel Y. Temporal and Spatial Assessment Of Fossil Fuel Sources Air Pollutants Using Remote Sensing and Spatial Data: A Case Study of Antalya Province Kepez. MSc Thesis, Akdeniz University, Antalya, Türkiye, 2024.
[19] Taka M, Salman M, Tuvar O, Utar A, Polat S. "Exploration of lignite in Konya Karapınar Neogene Basin". MTA, Ankara, Türkiye, 2009-33-13-01-2, 2010.
[20] Altunsoy M, Özçelik O, Hökerek S, Taka M. "The organic facies characteristics of the Pliocene units from south of the Karapınar (Konya)." Research Unit of the Akdeniz University, Antalya, Türkiye, 2010.02.0121.017, 2011.
[21] Özcan A, Göncüoglu MC, Turhan N, Sentürk K, Uysal S, Isık A. "Basement geology of Konya-Kadınhanı-Ilgın region". MTA, Ankara, Türkiye, 9535, 1990.
[22] Council of the European Communities. "Council directive 86/278/EEC of 12 June 1986 on the protection of the environment, and in particular of the soil, when sewage sludge is used in agriculture". *Official Journal,* L 181 (04.07.1986), 1986.
[23] Oskay RG, Christanis K. Inaner H, Salman M, Taka M. "Palaeoenvironmental reconstruction of the eastern part of the Karapınar-Ayrancı coal deposit (Central Turkey)". *International Journal of Coal Geology*, 163, 100-111, 2016.
[24] Dai SF, Finkelman RB, Hower JC, French D, Graham IT, Zhao L. *Inorganic Geochemistry of Coal*. Amsterdam, Netherlands, Elsevier, 2023.
[25] Ketris MP, Yudovich E. "Estimations of clarkes for carbonaceous biolithes: world average for trace element contents in black shales and coals". *International Journal of Coal Geology,* 78, 135–148, 2009.
[26] Rudnick RL, Gao S. *Treatise on Geochemistry, Volume 3*. Editors: Holland HD, Turekian KK. The Crust, Oxford, United Kingdom, Elsevier-Pergamon, 2003.
[27] Pandey VC, Singh JS, Singh RP, Singh N, Yunus M. "Arsenic hazards in coal fly ash and its fate in Indian scenario". *Resources, Conservation and Recycling*, 55(9-10), 819-835, 2011.
[28] Ruhl L, Vengosh A, Dwyer GS, Hsu-Kim H, Deonarine A, Bergin M, Kravchenko J. "Survey of the potential environmental and health impacts in the immediate aftermath of the coal ash spill in Kingston, Tennessee". *Environmental Science & Technology*, 43(16), 6326-6333, 2009.
[29] Finkelman R. "Potential human health impacts of burning coal beds and waste banks". *International Journal of Coal Geology,* 59, 19-24, 2004.
[30] Pesch B, Ranft U, Jakubis P, Nieuwenhuijsen MJ, Hergemöller A, Unfried K, Jakubis M, Miskovic P, Keegan T. "Environmental arsenic exposure from a coal-burning power plant as a potential risk factor for nonmelanoma skin carcinoma: results from a case-control study in the district of Prievidza, Slovakia". *American Journal of Epidemiology*, 155(9), 798-809, 2002.
[31] Swaine DJ, Goodarzi F. *Environmental Aspects of Trace Elements in Coal (Vol. 2).* Springer Science & Business Media, 1995.
[32] Kumari M, Kumar A, Bhattacharya T. "Assessment of heavy metal contamination in street dust: concentrations, bioaccessibility, and human health risks in coal mine and thermal power plant complex". *Environmental Geochemistry and Health*, 45, 7339-7362, 2023.
[33] Moreno T, Trechera P, Querol X, Lah R, Johnson D, Wrana A, Williamson B. "Trace element fractionation between PM10 and PM2.5 in coal mine dust: Implications for occupational respiratory health". *International Journal of Coal Geology*, 203, 52-59, 2019.